INTERPARTICLE MAGNETIC INTERACTIONS WITHIN A SINGLE DOMAIN MAGNETITE POWDER

Nikola VÍTKOVSKÁ[1], Petr JANDAČKA[1,2], Ondřej ŽIVOTSKÝ[1,3], Jiří LUŇÁČEK[1,3]

[1] *Institute of Physics, VSB-Technical University of Ostrava, 17. listopadu 15/2172, 70833 Ostrava, Czech Republic, nikola.vitkovska@vsb.cz, petr.jandacka@vsb.cz, ondrej.zivotsky@vsb.cz, jiri.lunacek@vsb.cz*

[2] *IT4Innovations Centre, VSB-Technical University of Ostrava, 17. listopadu 15/2172, 70833 Ostrava, Czech Republic*

[3] *Department 606, VSB-Technical University of Ostrava, 17. listopadu 15/2172, 70833 Ostrava, Czech Republic*

Abstract

The contribution presents interparticle magnetic interactions in dry ferrimagnetic single domain magnetite powder (the size of crystals being less than 50 nm) and in magnetite/magnesium oxide mixture powder (75 %, 50 % and 25 % of magnetite), where diamagnetic MgO powder is composed of micrometric grains. The study of magnetization of magnetite nanoparticles in diamagnetic matrices was motivated by similar structures discovered in biological systems. Intensity of interparticle interactions was measured using vibrating sample magnetometer Microsense EV9 and characterized by magnetization parameter $\Delta M = M_{vir} - 0.5(M_{up} + M_{down})$ in Henkel plots, where M_{vir} is value of virgin curve, and M_{up} and M_{down} are values of magnetization in positive external fields of magnetization curve. Pure magnetite powder exhibits typical negative (dipolar) interactions with the minimum of about 0.02 T at 20 °C, while at lower temperatures the interactions are stronger. Consequently, at temperature of -140 ºC the peak value moves up to 0.03 T. Partial substitution of magnetite by MgO significantly influences interparticle interactions. The intensity ΔM increases in comparison to 100 % magnetite powder, while the position of peaks does not change much and slowly fluctuates between about 0.01-0.02 T. Moreover, sample with 25 % of magnetite exhibits also positive exchange interactions at magnetic fields of above 0.1 T (maxima). Taking into account the three contributions of magnetic energy, magnetic anisotropy energy, Zeeman energy, and interparticle magnetic energy, such results can be explained in the context of an interparticle shielding effect, when particles in the powder are more densely arranged.

Keywords: magnetite nanoparticles, Henkel plot, single domain magnetite powder

1. INTRODUCTION

Iron rich structures were discovered in several biological systems containing especially magnetic minerals like magnetite, hematite, maghemite or ferrihydrite [1-7]. Since these minerals exhibit significant magnetic properties, speculations about their role in these organisms started. Typically they are superparamagnetic clusters of nanoparticles of the mentioned minerals. Also the single-domain form of magnetite in magnetotactic bacteria has been mineralogically well described [2]. Such clusters of biogenic particles that often have small volumes (the diameter of crystal clusters is smaller than 1 μm) are hard to analyze and determine their phase composition in a biological tissue. Often we can only detect significant content of Fe using EDX (Energy-Dispersive X-ray spectroscopy) spectra. In such case there is a possibility to identify these particles magnetically, best using some magnetic parameter that does not depend on the amount of magnetic material in the biological sample. Such possibility in the case of magnetite detection is offered, besides Verwey Transition [8] and First Order Reversal Curve method (FORC method) [9, 10], by the Henkel plot construction that describes the intensity of interparticle magnetic interactions in a measured sample [11, 12]. The goal of this contribution is to find significant magnetization points in the Henkel plot for single

domain magnetite. We have focused our attention on the influence of temperature and diamagnetic matrix on these interactions.

2. MATERIAL AND METHOD

A subject of measurement was a single domain magnetite (Fe_3O_4) powder provided by the Sigma Aldrich Company, product no. 637106, particle size smaller than 50 nm but larger than 20 nm (magnetite nanoparticles smaller than 20 nm are in superparamagnetic state) [13-15]. We have used a fine magnesium oxide (MgO) powder ground into a micrometric form as a diamagnetic matrix for magnetic particles. It was provided by the Sigma Aldrich Company, product no. 220361. For the measurements with a diamagnetic matrix we have prepared 4 types of samples, specifically: Samples with 100 % content of magnetite by volume, 75 % of magnetite (25 % percent is made up by MgO powder), 50 % of magnetite and 25 % of magnetite. These mixed samples were prepared by simple mechanic mixing of the two mentioned components in dry state. All powder samples were placed (compressed) to a small plastic vessel with the volume of 7.73×10^{-8} m^3. Afterward a sampler was attached to a glass sample holder to a magnetometer using a teflon tape. The influence of the glass holder and the attachment tape to magnetic measurements was negligible.

The magnetic measurements were done using the VSM EV9 Microsense vibration magnetometer with the magnetic moment resolution of 10^{-10} $A \cdot m^2$ and resolution of the magnetic field setting of 10^{-4} T. The construction of the Henkel plot consists of two measurements. It starts with the demagnetization of the sample in AC magnetic field, continues with the measurement of a virgin curve and ends with recording of a hysteresis loop [11]. Henkel plots of 100 % magnetite content were obtained not only at room temperatures, but also at lower temperatures. In this case the powders were cooled down using liquid and gaseous nitrogen to the constant temperatures – 140 °C, − 100 °C and – 50 °C. Estimated temperature deviation of temperature instability was approximately ± 5 °C.

3. THEORETICAL BACKGROUND

Interparticle magnetic interactions of powder samples composed of a single-domain, randomly oriented particles with magnetic anisotropy (the easy magnetization axis of magnetite is 111) [16], can be described by construction of the Henkel plot. It depicts the relation of magnetization deviation ΔM that expresses the intensity of interparticle interactions at an external magnetic field. The magnetic deviation is calculated using the equation:

$$\Delta M(B) = M_{vir}(B) - 0.5 \cdot [M_{up}(B) + M_{down}(B)], \quad (1)$$

where M_{vir} is the value of magnetization on a virgin curve at certain external magnetic field B, M_{up} and M_{down} are the values of magnetization during increase and decrease of a positive external field, respectively [11, 17]. An alternative method of the Henkel plot construction is based on measuring of the remnant magnetization as a function of an external magnetic field [11, 17], where the meaning of the ΔM value is the same for both methods. In the case that $\Delta M = 0$ $A \cdot m^2/g$ the sample does not exhibit interparticle interactions. For $\Delta M > 0$ $A \cdot m^2/g$ the exchange of coupling interactions between particles prevails, while for $\Delta M < 0$ $A \cdot m^2/g$ the magnetic dipole interactions are detected [12]. We use the unit $A \cdot m^2/$ (relative volume content of magnetite) or the magnetic moment unit $A \cdot m^2$ for practical reasons.

4. RESULTS

Fig. 1 shows the influence of temperature on interparticle interactions in the magnetite powder. It is apparent that the intensity of interactions gets to the extreme in the range of external fields 0.02 – 0.04 T. The highest intensity of interactions is observed at temperature -140 °C, further temperature increase causes shift of the extremes toward the lower magnetic fields. The shape of the Henkel plot is related to basic parameters of measured hysteresis loops. Temperature dependent changes in the coercive field B_c, saturation

magnetization M_s, and remnant magnetization M_r are shown in Table 1 - left. It is obvious that increasing temperature diminishes these parameters.

Table 1 Magnetic parameters of the hysteresis loops. Influence of the temperature (left) and the concentration of magnetite in sample (right) on basic magnetization parameters.

Temp. (°C)	B_c (mT)	M_s (kA/m)	M_r (kA/m)
-140	18.0	102	23.1
-100	15.0	100	20.4
-50	11.0	97.0	16.2
20	7.3	92.4	12.1

Magnetite conc. (%)	B_c (mT)	M_s (kA/m)	M_r (kA/m)
100	7.3	92.4	12.1
75	2.3	90.4	64.7
50	7.6	82.0	11.6
25	6.9	94.3	13.5

Note: Magnetization values are related to volume of magnetite in samples.

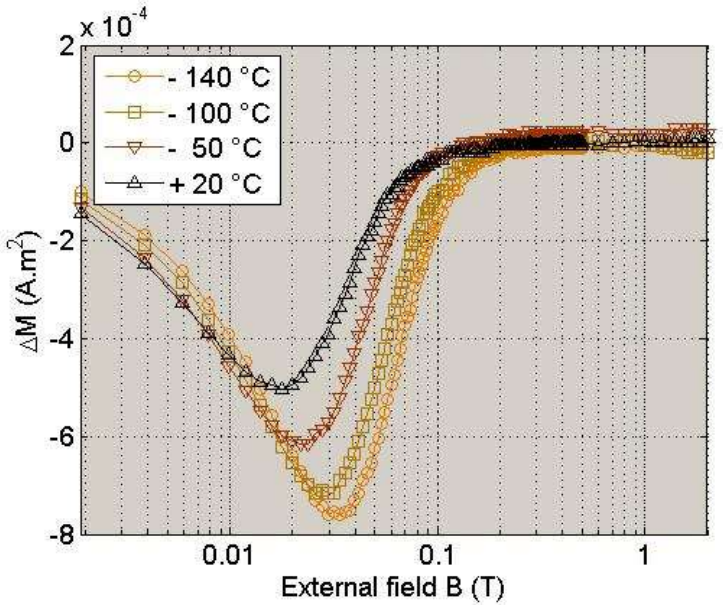

Fig. 1 The Henkel plots. The influence of temperature on interparticle interactions in the powder that consists of particles of single domain magnetite (particle size is smaller than 50 nm).

Fig. 2 shows behavior of the magnetite in a diamagnetic matrix. Henkel plots illustrate that all mixtures have the interaction extreme between the external fields 0.01 – 0.02 T. Although the results do not have an equivocal trend we can say that a diamagnetic matrix makes interparticle interactions more intensive, because the ΔM value gets to its maximum in the sample with 25 % Fe_3O_4. This result seems to be a paradox, since the magnetic dipole interaction energy should increase according to the expression $1/d^3$, where d is mutual separation of particles [18]. Moreover, the magnetization deviation ΔM in 25 % Fe_3O_4 turns to positive values at the magnetic field above 0.1 T. This indicates significant interparticle magnetic exchange coupling in the sample. Similarly as behavior of extremes in the Henkel plots, basic magnetization

parameters of the measured hysteresis loops shown in dependence on the magnetite concentration (see Table 1 - right) have also unclear trend.

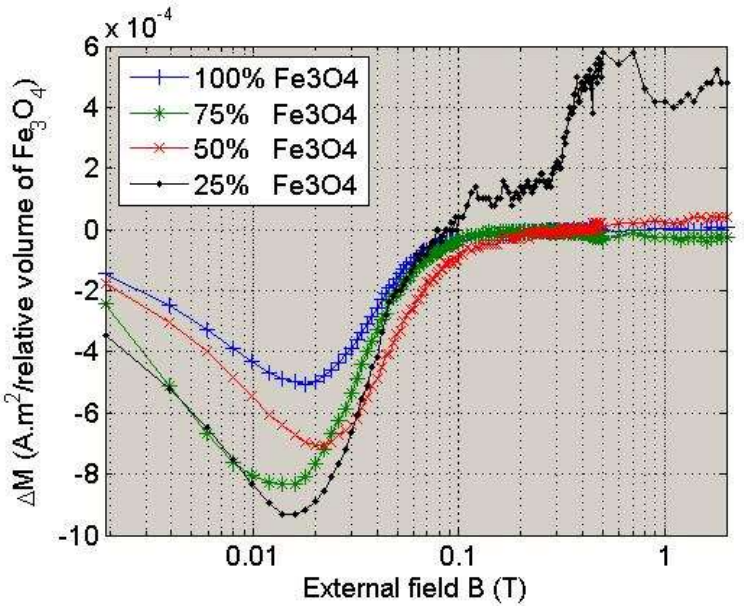

Fig. 2 The Henkel plots. The influence of diamagnetic matrix composed from fine MgO powder on interparticle magnetic interactions in single domain magnetite (particle size smaller than 50 nm).

5. DISCUSSION

The understanding of achieved results presented in Henkel plots must arise from phenomenological models of small magnetic particles behavior in an external magnetic field [12]. The basic theoretical approach that describes behavior of such particles is the Stoner-Wohlfarth model [19]. The energy description of the problem helps to understand extreme values in the Henkel plot. A total Gibbs energy G of the powder particle can be written in the form:

$$G = E_Z + E_D + E_K + E_{ex}, \quad (2)$$

where energy constituents are: $E_Z \sim M_s B \cdot \cos(\alpha - \beta)$ is the Zeeman energy, $E_D \sim m^2/d^3$ is the dipolar interaction energy between particles, $E_K \sim K \cdot \sin^2(\beta)$ is the anisotropy energy and $E_{ex} \sim \sum J \cdot S_i S_j$ describes the exchange coupling energy. Parameters are defined in the following way: M_s is the saturation magnetization, B is the external magnetic field, α is the angle between B and easy axis, β is the angle between M_s and the easy axis, m is the magnetic moment of particle, d is the separation of two particles, K is the magnetic anisotropy constant, J is the exchange integral and S_i and S_j are electron spins of two different particles [12, 18-20]. The energies E_D and E_{ex} thus represent interparticle magnetic interactions. The Gibbs energy depends on the intensity of the external magnetic field. During magnetization process a powder energy spontaneously drops to minimum, which can be derived from the equation (2) using condition $dG/dB = 0$. The relation between equations (1) and (2) is given by the relationship between magnetization **M** and the volume density of magnetic energy in the space ε (J/m^3), where $\varepsilon = 0.5 \cdot \mathbf{B_t H}$. Total magnetic induction $\mathbf{B_t}$ is equaled to $\mathbf{B} + \mathbf{B_i} = \mu_0(\mathbf{H} + \mathbf{M})$, where **H** is the intensity of magnetic field in the vacuum, $\mathbf{B_i}$ is the internal magnetic induction, **B** is the external magnetic induction and μ_0 is the vacuum permeability [20, 21]. Positive or negative values of ΔM are given by predominating magnetic energy at specific external magnetic field.

Fig. 1 shows that increasing temperature T lowers the value ΔM. This is an expected result, because material magnetic parameters depend on temperature. Increasing thermal energy kT, where k is the Boltzmann constant, causes a weakening and consequently breakage the magnetic domain structure of crystals. As a result the intensity of negative dipole interactions slowly decreases in the magnetite powder.

As was mentioned before, increase of negative interactions with decreasing concentration of magnetite (Fig. 2) is surprising. Moreover, in the case of the sample with 25 % Fe_3O_4 transition to positive values of ΔM above 0.1 T is evident. We suppose that these effects are connected with preparation of samples, for example due to inhomogeneous distribution of particles in the sample. On the other hand, there is also a big difference between particle size of MgO matrix (100 nm – 100 μm) and magnetic nanoparticle Fe_3O_4 (less than 50 nm). Mixing of both materials can lead to the formation of gaps among MgO particles. Therefore, higher content of the diamagnetic matrix in the sample causes increase of gap numbers, what is probably responsible for pseudo-positive exchange coupling interactions observed in the sample with 25 % Fe_3O_4. In this sample density of gaps can induce migration and rotation of Fe_3O_4 particles at the sufficient high magnetic fields (more than 0.1 T). We expect that these parasitic effects in our measurements can be eliminated by the different method of sample preparation, namely by pressing powder samples into the form of tablets. This procedure would limit translation and rotation movement of particles within the sample invoked at the higher external magnetic field.

CONCLUSION

In the paper we analyzed Henkel plots of the single domain magnetite powder and the magnetite/magnesium oxide mixture powder. Magnetic fields at which the Henkel plot exhibits the extreme are approximately in the range from 0.01 to 0.04 T and are weakly depending on the temperature and concentration of the magnetite. On the other hand, intensity of interactions is strongly dependent on both mentioned parameters and decreases with increasing temperature and magnetite concentration. Behavior of the sample with low concentration of the magnetite (25 %), that exhibits positive interparticle interactions, would also deserve further analysis and testing of results. In the future, such type of interactions could belong to significant markers of single domain magnetite nanoparticles in biological or mineralogical natural samples. Conclusively, validity of magnetic measurements on nanopowders is strongly depending on the sample preparation technique. In further work we are going to work with the samples in form of tablets that will be prepared by the mechanical compression method using a non-magnetic brass die.

ACKNOWLEDGEMENTS

Authors would like to thank for financial support via projects: 1) Student grant competition project, reg. no. SP 2014/27, 2) IT4Innovations, reg. no. CZ.1.05/1.1.00/02.0070, 3) RMTVC, reg. no. CZ.1.05/2.1.00/01.0040

REFERENCES

[1] BAZYLINSKI, D. A., FRANKEL, R. B. Magnetosome formation in prokaryotes. *Nature Reviews Microbiology*, 2004**,** vol. 2, n. 3, pp. 217-230.

[2] FAIVRE, D., SCHULER, D. Magnetotactic Bacteria and Magnetosomes. *Chemical Reviews,* 2008**,** vol. 108, n. 11, pp. 4875-4898.

[3] FLEISSNER, G., HOLTKAMP-ROTZLER, E., HANZLIK, M., WINKLHOFER, M., FLEISSNER, G., PETERSEN, N., WILTSCHKO, W. Ultrastructural analysis of a putative magnetoreceptor in the beak of homing pigeons. *Journal of Comparative Neurology,* 2003**,** vol. 458, n. 4, pp. 350-360.

[4] HANZLIK, M., HEUNEMANN, C., HOLTKAMP-ROTZLER, E., WINKLHOFER, M., PETERSEN, N., FLEISSNER, G. Superparamagnetic magnetite in the upper beak tissue of homing pigeons. *Biometals,* 2000**,** vol. 13, n. 4, pp. 325-331.

[5] HSU, C. Y., KO, F. Y., LI, C. W., FANN, K., LUE, J. T. Magnetoreception System in Honeybees (Apis mellifera). *Plos One,* 2007**,** vol. 2, n. 4.

[6] HSU, C. Y., CHAN, Y. P. Identification and Localization of Proteins Associated with Biomineralization in the Iron Deposition Vesicles of Honeybees (Apis mellifera). *Plos One* 2011**,** vol. 6, n. 4.

[7] GOULD, J. L., KIRSCHVINK, J. L., DEFFEYES, K. S. Bees Have Magnetic Remanence. *Science,* 1978**,** vol. 201, n. 4360, pp. 1026-1028.

[8] LI, J. H., WU, W. F., LIU, Q. S., PAN, Y. X. Magnetic anisotropy, magnetostatic interactions and identification of magnetofossils. *Geochemistry Geophysics Geosystems,* 2012**,** vol. 13.

[9] SCHREFL, T., SHOJI, T., WINKLHOFER, M., OEZELT, H., YANO, M., ZIMANYI, G. First order reversal curve studies of permanent magnets. *Journal of Applied Physics,* 2012**,** vol. 111, n. 7.

[10] GILBERT, D. A., ZIMANYI, G. T., DUMAS, R. K., WINKLHOFER, M., GOMEZ, A., EIBAGI, N., VICENT, J. L., LIU, K. Quantitative Decoding of Interactions in Tunable Nanomagnet Arrays Using First Order Reversal Curves. *Scientific Reports,* 2014, vol. 4.

[11] THAMM, S., HESSE, J. A simple plot indicating interactions between single-domain particles. *Journal of Magnetism and Magnetic Materials* 1996**,** vol. 154, n. 2, pp. 254-262.

[12] ZHANG, H. W., RONG, C. B., DU, X. B., ZHANG, J., ZHANG, S. Y., SHEN, B. G. Investigation on intergrain exchange coupling of nanocrystalline permanent magnets by Henkel plot. *Applied Physics Letters,* 2003**,** vol. 82, n. 23, pp. 4098-4100.

[13] MUXWORTHY, A. R., WILLIAMS, W. Critical superparamagnetic/single-domain grain sizes in interacting magnetite particles: implications for magnetosome crystals. *Journal of the Royal Society Interface,* 2009**,** vol. 6, n. 41, pp. 1207-1212.

[14] MUXWORTHY, A. R., WILLIAMS, W. Critical single-domain/multidomain grain sizes in noninteracting and interacting elongated magnetite particles: Implications for magnetosomes. *Journal of Geophysical Research-Solid Earth,* 2006**,** vol. 111, n. B12.

[15] PANKHURST, Q. A., CONNOLLY, J., JONES, S. K., DOBSON, J. Applications of magnetic nanoparticles in biomedicine. *Journal of Physics D-Applied Physics,* 2003**,** vol. 36, n. 13, pp. R167-R181.

[16] KAKOL, Z., KROL, G., TABIS, W., KOLODZIEJ, T., WISNIEWSKI, A., STEPANKOVA, H., CHLAN, V., KUSZ, J., TARNAWSKI, Z., KOZLOWSKI, A., HONIG, J. M. Easy axis switching in magnetite. *Joint European Magnetic Symposia (Jems),* 2011**,** vol. 303.

[17] THAMM, S., HESSE, J. The remanence of a Stoner-Wohlfarth particle ensemble as a function of the demagnetisation process. *Journal of Magnetism and Magnetic Materials,* 1998**,** vol. 184, n. 2, pp. 245-255.

[18] MORUP, S., HANSEN, M. F., FRANDSEN, C. Magnetic interactions between nanoparticles. *Beilstein Journal of Nanotechnology,* 2010**,** vol. 1, pp. 182-190.

[19] STONER, E. C., WOHLFARTH, E. P. A Mechanism of Magnetic Hysteresis in Heterogeneous Alloys. *Philosophical Transactions of the Royal Society of London Series a-Mathematical and Physical Sciences,* 1948**,** vol. 240, n. 826, pp. 599-642.

[20] KITTEL, C., *Introduction to Solid State Physics*. Wiley, 2004.

[21] AHARONI, A. Magnetostatic Energy Calculations. *Ieee Transactions on Magnetics,* 1991**,** vol. 27, n. 4, pp. 3539-3547.